

1 **Article can be downloaded under:**

2 **<http://dx.doi.org/10.1016/j.fuel.2015.06.085>**

3

4 **Techno-economic Study of the Storage of Fluctuating Renewable**  
5 **Energy in Liquid Hydrocarbons**

6 *Daniel H. König, Marcel Freiberg, Ralph-Uwe Dietrich, Antje Wörner*

7 German Aerospace Center, Institute of Engineering Thermodynamics, Pfaffenwaldring 38-40, 70569  
8 Stuttgart, Germany

9 **Corresponding Author**

10 German Aerospace Center  
11 Institute of Engineering Thermodynamics  
12 Daniel H. König  
13 Pfaffenwaldring 38-40  
14 70569 Stuttgart  
15 Germany  
16 Phone: 0049 711 6862-673

17 Email: [daniel.koenig@dlr.de](mailto:daniel.koenig@dlr.de)

18

19 KEYWORDS: Renewable energy, Energy storage, Fischer-Tropsch synthesis, Techno-economic

20 Analysis, Synthetic fuels

21

22 ABSTRACT

23 Liquid hydrocarbons are considered as an option to store renewable energy while decoupling the supply  
24 and demand of renewable resources. They can also be used as transportation fuel or as feedstock for the  
25 chemical industry and are characterized by a high energy density. A process concept using renewable  
26 energy from fluctuating wind power and CO<sub>2</sub> to produce liquid hydrocarbons was modeled by a  
27 flowsheet simulation in Aspen Plus®. The capacity of the plant was set to 1  $GW_{LHV}$  of hydrogen input,  
28 using water electrolysis, reverse-water-gas-shift reaction (RWGS) and Fischer-Tropsch (FT) synthesis.  
29 A feed of 30 *t/h* of H<sub>2</sub> generated 56.3 *t/h* (12,856 *bbl/d*) of liquid hydrocarbons. A Power-to-Liquid  
30 efficiency of 44.6 % was calculated for the base case scenario. Net production cost ranged from  
31 12.41  $\$/GGE$  to 21.35  $\$/GGE$  for a system powered by a wind power plant with a full load fraction of  
32 about 47 %, depending on the assumed electricity feedstock price and electrolyzer capital cost. For  
33 systems with full load fractions between 70 % and 90 %, the production cost was in the range of  
34 5.48  $\$/GGE$  to 8.03  $\$/GGE$ .

## 35 **1. Introduction**

36 In 2012, a total of 1,133 *TWh* of renewable power was generated worldwide, corresponding to 5.0 % of  
37 the total electricity generated [1]. Depleting, finite fossil fuel reserves and the goal to reduce CO<sub>2</sub>  
38 emissions led to a transition to alternative power generation technologies. Therefore, an increasing  
39 number of renewable energy installations is now being observed. It is predicted that from 2014 to 2035,  
40 the renewable generation capacity will double to about 3,930 *GW* of installed capacity [2]. Over the past  
41 decade, conventional power plants accounted for about 68 % of the investment in the power sector. By  
42 2035, however, about 62 % of the investment is predicted to be in renewable technologies [2].

43 In conventional energy systems, power generation follows the energy demand [3]. In contrast, wind and  
44 solar power generation follows natural conditions, with hourly, daily, weekly or seasonal fluctuations  
45 [4]. Hence, long-term seasonal storage applications with a high capacity, low storage losses, well-  
46 established and safe storage tanks and low space requirements are required. Liquid hydrocarbons are  
47 considered an option to store renewable energy while decoupling supply and demand. They are  
48 characterized by a high energy density, are used in the transportation sector and exhibit little to no loss  
49 during long-term storage. Additionally, liquid hydrocarbons have an existing infrastructure, can be  
50 easily transported and also be used as transportation fuel or as feedstock for the chemical industry.

51 The generation of liquid hydrocarbons was investigated by several studies [5], [6], [7], [8] and [9].  
52 Current research focuses on the optimization of the generation of fuels and olefins from biomass and  
53 natural gas [10]. On the other hand, the use of CO<sub>2</sub> for the production of synthetic fuels demonstrates a  
54 real greenhouse gas sink. This technology combines CO<sub>2</sub>/steam-mixed reforming and CO<sub>2</sub>-active iron  
55 catalysts in Fischer-Tropsch synthesis in Gas-to-Liquid processes [11]. The generation of liquid  
56 transportation fuels by combining a solid oxide electrolyzer cell and Fischer-Tropsch (FT) synthesis was  
57 investigated by [6] and [7]. Mignard et al. investigated the generation of alcohols from marine energy  
58 and CO<sub>2</sub> [5]. Jess et al. suggest generating liquid fuels from solar energy and CO<sub>2</sub> [8]. A rating of  
59 several Power-to-Liquid (PtL) technologies was proposed by Tremel et al [9]. The aforementioned  
60 references assume a continuous supply of energy and reactant to the fuel production plant.

61 The present work investigates the techno-economic effect of an option to couple continuous fuel  
62 production with fluctuating energy sources, considering present realistic assumptions and future  
63 technological developments.

64 The economic potential of storing fluctuating renewable energy in liquid hydrocarbons is of special  
65 interest for renewable power station operators and for the prediction of future energy scenarios.  
66 Renewable liquid hydrocarbons may contribute to the fuel supply for aviation as well [12]. A techno-  
67 economic study was carried out, starting with a detailed process model of the generation of liquid  
68 hydrocarbons by FT synthesis. The model was analyzed by pinch point analysis and the economic  
69 performance was estimated on the basis of capital and operation cost estimations.

## 70 **2. Scope of Evaluation and Process Description**

71 The evaluation focuses on the production of liquid hydrocarbons from renewable excess power and CO<sub>2</sub>.  
72 The system boundary and the block flow diagram of the process concept are shown in **Fehler!**  
73 **Verweisquelle konnte nicht gefunden werden.**

74 The focus on fluctuating renewable energy requires a highly flexible electrolyzer unit. A proton  
75 exchange membrane (PEM) electrolyzer can be operated at high current densities (above 2 A/cm<sup>2</sup>) and  
76 cover a nominal power density range from 10 % to 100 % [13]. A storage cavern acts as the link  
77 between the highly fluctuating source, the electrolyzer unit and the continuous chemical synthesis.  
78 Hydrogen is stored if excess power is available and used when the hydrogen demand exceeds its  
79 generation. The liquid product is stored in tanks for later use. The economic analysis comprises the cost  
80 estimation for the electrolyzer unit, the hydrogen storage cavern and the chemical plant, including  
81 auxiliary units and utilities.

82 **Fehler! Verweisquelle konnte nicht gefunden werden.** illustrates a more detailed flowsheet of the  
83 process concept. The PEM electrolysis and the cavern are not modeled in the flowsheet. The capacity of  
84 the plant is set to 1 GW of hydrogen input based on its lower heating value (LHV). H<sub>2</sub> from electrolysis  
85 and CO<sub>2</sub>, which is delivered by a pipeline, are fed to the plant. CO<sub>2</sub> and H<sub>2</sub> are converted in the reverse-  
86 water-gas-shift (RWGS) reactor to syngas, which is composed of H<sub>2</sub> and CO. The syngas is then further

87 converted to hydrocarbons in the FT synthesis. The hydrocarbon syncrude is upgraded and separated  
88 from unreacted feed and gaseous hydrocarbons to make the final product.

### 89 3. Simulation Model

90 A flowsheet simulation model was developed in Aspen Plus®. Heat losses of reactors, heat exchangers  
91 and piping were neglected. Furthermore, the electrolyzer and the storage cavern are not included in the  
92 flowsheet model. The pressure losses in the process are lumped in the recycle stream and are assumed to  
93 be 0.2 MPa [14].

#### 94 3.1. Components and thermodynamic model

95 The model is based on the pure components H<sub>2</sub>, CO<sub>2</sub>, CO, and H<sub>2</sub>O and the n-alkanes CH<sub>4</sub> through to  
96 C<sub>30</sub>H<sub>62</sub>, which were selected from the Aspen database. Coke is represented by solid carbon.  
97 Hydrocarbon products are represented only by n-alkanes, since the main products of cobalt based low  
98 temperature FT synthesis are n-alkanes [15]. CH<sub>4</sub> through to C<sub>4</sub>H<sub>10</sub> are gases, C<sub>5</sub>H<sub>12</sub> through to C<sub>20</sub>H<sub>42</sub>  
99 are liquids and hydrocarbons with a chain length longer than C<sub>20</sub> are waxes. In this work, the Peng-  
100 Robinson equation of state in combination with the Boston-Mathias alpha function is used to describe  
101 the phase behavior in the process [16], [17]. The Peng-Robinson equation of state is widely applied in  
102 gas processes, refining and FT modeling studies [14], [18], [19].

#### 103 3.2. Reverse water-gas-shift reactor

104 The reverse water-gas-shift (RWGS) reaction (1) is the endothermic hydrogenation of CO<sub>2</sub> to CO [20].



106 The RWGS reactor model comprises a Gibbs energy minimization reactor model and an adiabatic  
107 burner model. The Gibbs energy minimization reactor model assumes thermodynamic equilibrium for  
108 the RWGS, which is a reasonable assumption at high temperatures [8], [20]. The operation temperature  
109 and pressure are assumed to be 900 °C and 2.5 MPa, respectively [21]. In addition to the fresh feed, the  
external recycle (see **Fehler! Verweisquelle konnte nicht gefunden werden.**) is fed to the RWGS

110 reactor. The external recycle contains unreacted reactants and gaseous hydrocarbons from the FT  
 111 synthesis. Hence, steam reforming of the gaseous hydrocarbons occurs as a side reaction in the RWGS  
 112 reactor. The external recycle is a split of the total recycle (from flash F-5, see **Fehler! Verweisquelle**  
 113 **konnte nicht gefunden werden.**), whose split fraction is determined by the fuel demand of the burner  
 114 (FG-1). The adiabatic burner model supplies heat to the RWGS reactor.

115 To reduce coking in the reformer, the carbon safety factor (CSF) was introduced [14], [22]. The CSF  
 116 determines the amount of steam required to achieve a constant distance from the coking equilibrium.  
 117 The CSF is calculated by equations (2) and (3).

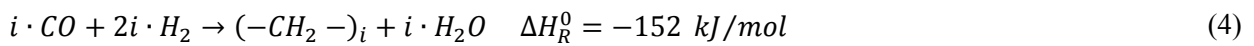
$$CSF = \frac{y_{CO_2}}{y_{CO}^2} \cdot \frac{1}{P} \cdot K(T) \quad (2)$$

$$K(T) = e^{-\frac{\Delta G_R^0(T_0)}{R \cdot T_0} - \frac{\Delta H_R^0(T_0)}{R} \left(\frac{1}{T} - \frac{1}{T_0}\right)} \quad (3)$$

118  $y_{CO_2}$  and  $y_{CO}$  are the molar fraction of  $CO_2$  and  $CO$ , respectively.  $P$  is the overall pressure and  $K(T)$  the  
 119 temperature dependent equilibrium constant.  $K(T)$  is calculated by the Gibbs reaction enthalpy ( $\Delta G_R^0$ ),  
 120 the reaction enthalpy ( $\Delta H_R^0$ ), the ideal gas constant  $R$ , the temperature  $T$  and the standard temperature  
 121  $T_0 = 25^\circ C$ . To achieve an O/C ratio greater than 2, the criterion  $CSF = 3$  must be met.

### 122 3.3. Fischer-Tropsch synthesis

123 In FT synthesis,  $CO$  and  $H_2$  are polymerized to long chain hydrocarbons over a catalyst (4).



124 The chain growth probability,  $\alpha$ , is a measure if whether chain propagation or termination occurs (5)  
 125 and is connected to the weight fraction,  $w_n$ , by the Anderson-Schulz-Flory distribution [15], which  
 126 determines the product distribution.

$$w_n = \frac{(1 - \alpha)}{\alpha} \cdot \alpha^n \cdot n \quad (5)$$

127 The reaction scheme of a cobalt-based catalyst at low temperatures was selected for this work, since the  
128 yield of n-alkanes is high for this kind of catalyst [15], [23]. The FT synthesis was modeled by a  
129 stoichiometric reactor model. The model comprises 30 reactions for the generation of hydrocarbons  
130 from CH<sub>4</sub> to C<sub>30</sub>H<sub>62</sub>. The molar fractional conversion of each reaction is determined by  $\alpha$ , the corrected  
131 methane yield and the per-pass conversion of CO as displayed in the supplementary information (SI)  
132 Table S1. The H<sub>2</sub>-to-CO ratio, the molar fraction of the reactants and the operation temperature and  
133 pressure are fixed and also reported in Table S1 (of the SI). The ratio of H<sub>2</sub> feed to CO<sub>2</sub> feed is adjusted  
134 to meet the H<sub>2</sub>-to-CO ratio criteria. The molar fraction of the reactants is adjusted by the internal recycle,  
135 which is determined by the amount of gaseous product taken from the fourth flash (F-4).

### 136 *3.3. Product separation and upgrading section*

137 The targeted products of the plant are liquid hydrocarbons with a chain length ranging from C<sub>5</sub> to C<sub>20</sub>.  
138 Therefore, hydrocracking is required to crack the waxes into shorter chain hydrocarbons in the desired  
139 range. The hydrocracker model is based on a yield distribution [24]. It operates at 6.0 MPa and  $T_{HC} =$   
140 350 °C. A five step product separation section is modeled to represent the separation of liquid products  
141 from the gaseous byproducts, reaction water, unreacted gases and inserts [15]. The separation  
142 temperatures are:  $T_{F-1} = 145^{\circ}C$ ,  $T_{F-2} = 100^{\circ}C$ ,  $T_{F-3} = 100^{\circ}C$ ,  $T_{F-4} = 10^{\circ}C$  and  $T_{F-5} = -30^{\circ}C$ . The  
143 liquid products of the separation stages F-2 through to F-5 are collected and brought together with the  
144 product of the hydrocracker to ambient conditions in the flash drum F-6. The gaseous byproduct is  
145 additional fuel for the burner.

## 146 **4. Model Results and Process Performance**

### 147 *4.1. Model results*

148 The operation parameters of the 1 GW<sub>LHV</sub> H<sub>2</sub> input plant are described in the simulation model section.  
149 About 270 t/h of H<sub>2</sub>O and 236 t/h of CO<sub>2</sub> are required to generate about 56 t/h of liquid  
150 hydrocarbons. The mass flow block diagram is displayed in Figure S1 of the supplementary information  
151 (SI). The main share of the liquid hydrocarbon product is in the range of C<sub>5</sub> to C<sub>10</sub>. The detailed product  
152 distribution is shown in Figure S2 in the SI.



153

#### 154 4.2. Heat integration

155 The cooling and heating requirements are determined by pinch point analysis. The composite curves are  
156 shown in **Fehler! Verweisquelle konnte nicht gefunden werden.** and indicate that the heating demand  
157 of the process can be satisfied by internal heat exchange. A total cooling demand of 431.5 MW must be  
158 realized to cool down the remaining hot streams of the process. Refrigeration, chilling and cooling water  
159 are selected as cooling utilities. A detailed record of the selected utility types, their characteristics and  
160 thermal loads is listed in Table S2 of the SI.

#### 161 4.3. Process performance

162 Five parameters are used to assess the process performance: three process efficiencies, a chemical  
163 conversion and a recycle ratio (see **Fehler! Verweisquelle konnte nicht gefunden werden.**). The  
164 chemical conversion efficiency,  $\eta_{CCE}$ , accounts for losses when converting H<sub>2</sub> and CO<sub>2</sub> into liquid  
165 hydrocarbons. The plant efficiency,  $\eta_{Plant}$ , considers the in-plant losses due to compression, pumping  
166 and utilities ( $P_U$ ). The Power-to-Liquid efficiency,  $\eta_{PtL}$ , relates the total energy input to the chemical  
167 energy content of the liquid products and considers the energy demand for electrolysis and AC/DC  
168 conversion. The carbon conversion,  $\eta_C$ , is a measure of the overall conversion of carbon atoms into  
169 hydrocarbons. The recycle ratio allows the evaluation of the size of the recycle streams. **Fehler!**  
170 **Verweisquelle konnte nicht gefunden werden.** summarizes the five process performance parameters  
171 and their respective calculation formulae.

172 The energy demand of electrolyzing water to hydrogen is predicted to be 4.3 kWh/Nm<sup>3</sup> for large-scale  
173 electrolyzer systems [25]. Thereby, the power demand for electrolysis is calculated as 1,450 MW.  
174 Assuming a conversion efficiency of 96 % for the AC/DC conversion, the power input to the process is  
175 calculated as 1,512 MW. The electrical demand for chilling and refrigeration results from the respective  
176 thermal loads and coefficients of performance. **Fehler! Verweisquelle konnte nicht gefunden werden.**  
177 summarizes the results of the flowsheet simulation. Additionally, the results of the performance  
178 parameters are shown.

179 The plant efficiency  $\eta_{plant}$  of 65.9 % is lower than the reported value of 69.3 % [9], which was  
180 calculated based on an idealized reaction scheme of 100 % conversion. The Power-to-Liquid efficiency  
181  $\eta_{PtL}$  of 44.6 % is lower than the reported value of 51 % [6], where instead of a PEM electrolyzer a solid  
182 oxide electrolyzer is applied, which uses excess heat directly to decrease the energy losses due to  
183 electrolysis. Apart from the liquid hydrocarbons, about 431.6 t/h (184 MW) of steam is produced as a  
184 byproduct.

## 185 **5. Economic Analysis**

186 A cost estimation was carried out for the proposed concept. The cost basis is the US dollar (\$, December  
187 2014).

### 188 *5.1. Methodology and results*

189 Methodology and accuracy comply with classes three and four of the Association for the Advancement  
190 of Cost Engineering for cost estimation in the process industry [26].

191 The component prices are estimated by equation (6) according to [27] and [28]. Scaling factors account  
192 for the economies of scale. Prices from previous years are updated via the Chemical Engineering Plant  
193 Cost Index (CEPCI).

$$PC = PC_{ref} \cdot \left(\frac{S}{S_{ref}}\right)^D \cdot \left(\frac{CEPCI_{2014}}{CEPCI_{ref}}\right) \cdot F \cdot z(S_{max}) \quad (6)$$

194 The equation gives the purchased cost ( $PC$ ) of equipment at the scale ( $S$ ) required for the proposed  
195 capacity in the year 2014.  $PC_{ref}$  is the purchased cost in the reference year at the reference scale ( $S_{ref}$ ).

196 The scaling factor ( $D$ ) accounts for scaling effects.  $CEPCI_{2014} = 576.1$  and  $CEPCI_{ref}$  are the cost  
197 indices for the year 2014 and the reference year, respectively [27], [29].  $F$  is a factor accounting for high  
198 pressure and special materials, where applicable. The quantity ( $z$ ) is the number of parallel trains  
199 dependent on the maximum scale  $S_{max}$ .

200 The installed capacity of the electrolyzer and the H<sub>2</sub> cavern depends on the fluctuating renewable power  
201 production pattern. Therefore, the electrolyzer capacity is calculated based on the amount of H<sub>2</sub> required  
202 per year and the full-load fraction of the fluctuating renewable energy source. An offshore wind power  
203 plant in the North Sea is selected as the fluctuating renewable energy scenario [30]. The wind pattern  
204 shows short-term and seasonal fluctuations from 0.03 GW to 3.2 GW (see Figure S3 of the SI). Based  
205 on the generation pattern, an annual full-load fraction of 46.8 % is calculated, which leads to a required  
206 electrolyzer capacity of 3.2 GW; the capacity of the cavern is calculated to 29.1 kt, or equivalent to  
207 11 % of the annual H<sub>2</sub> consumption. The filling level of the cavern is shown in Figure S3 of the SI. Due  
208 to the fluctuating pattern of power generation, the cavern must be partially filled for the start-up.  
209 Assuming that the same wind pattern applies each year, the required start-up amount of hydrogen is  
210 determined to be 22.5 kt.

211 **Fehler! Verweisquelle konnte nicht gefunden werden.** lists the capacities of the main components and  
212 the respective parameters required to calculate the purchased cost. The prices of the other process  
213 equipment are based on literature values [28].

214 The total purchased cost (TPC) of the plant is 3,150 M\$. The TPC is multiplied by ratio factors to  
215 account for installation, instrumentation, piping, electrical systems, buildings, yard improvements and  
216 service facilities [28]. Adding engineering, construction, legal expenses and contractor's fees, the fixed  
217 capital investment (FCI) for the chemical plant can be calculated by (7). The reported cost for the  
218 electrolyzer includes instrumentation, piping, electrical systems, service facilities, engineering and  
219 construction. Hence, the FCI of the electrolyzer is calculated by (8).

$$FCI_{Chemical\ Plant} = 4.60 \cdot TPC_{Chemical\ Plant} \quad (7)$$

$$FCI_{Electrolyzer} = 1.83 \cdot TPC_{Electrolyzer} \quad (8)$$

220 Including contingencies, working capital and the start-up expenses for the cavern, the total capital  
221 investment (TCI) is 8,690 M\$ (9). The start-up expenses for the cavern are 158 M\$.

$$TCI = 1.25 \cdot FCI_{Total} + Cost_{start-up\ cavern} \quad (9)$$

222 Assuming an interest rate of 7 % and a life time of 30 years for the electrolyzer unit and the chemical  
 223 plant, as well as 80 years for the cavern, the annualized capital cost (ACC) is calculated as 560 M\$/a  
 224 by (10) [27].

$$ACC = FCI \cdot \frac{IR \cdot (1 + IR)^{PL}}{(1 + IR)^{PL} - 1} \quad (10)$$

225 The operation costs are the costs for maintenance, insurance, taxes, reactants, materials, utilities and  
 226 revenues for byproducts. The maintenance cost for the chemical plant components is assumed to be 7 %  
 227 of FCI of the chemical plant [28]. The maintenance effort for the electrolyzer is calculated based on the  
 228 reconditioning period, which is reported to be 15 % of the FCI of the electrolyzer unit and must be  
 229 carried out every 60,000 hours of operation [31]. Insurance and taxes are 2 % of the overall FCI [28].  
 230 The prices for utilities, reactants and byproducts are listed in Table S3 in the SI.

231 The total operation cost (TOC) is 2,800 M\$/a. The total annualized cost (TAC) is the sum of the TOC  
 232 and the ACC. The net production cost (NPC) is 18.62 \$/GGE (6.83 \$/kg, 4.51 \$/l). Water electrolysis  
 233 and intermediate storage in the cavern account for about 89 % of the NPC.

234 **Fehler! Verweisquelle konnte nicht gefunden werden.** depicts the distribution of the total capital  
 235 investment and the net production cost on the different cost categories. With all of the above mentioned  
 236 realistic assumptions for an 1 GW<sub>LHV</sub> H<sub>2</sub> input PtL plant, the annual capital cost and the cost for  
 237 electricity to power the electrolysis account for about 85 % of the net production cost.

## 238 5.2. Sensitivity analysis

239 The effect of several economic parameters on the production cost of liquid hydrocarbons is shown in  
 240 **Fehler! Verweisquelle konnte nicht gefunden werden..** The steeper the slope is, the larger the  
 241 parameter's effect on the overall economics is. **Fehler! Verweisquelle konnte nicht gefunden werden.**  
 242 shows that both the capital cost of the electrolyzer and the cost of electricity have the highest slopes. As  
 243 shown in **Fehler! Verweisquelle konnte nicht gefunden werden.**, these are the cost categories with the

244 highest share of the production cost. If offshore wind power was available for half of the assumed  
245 186  $\$/MWh$ , the NPC would shrink to 11.81  $\$/GGE$ . Assuming excess power free of charge, the NPC  
246 drops to 5.00  $\$/GGE$ . The effect on the revenues due to selling  $O_2$  has a larger impact on the production  
247 cost than the purchase of  $CO_2$ . The effect of changing the costs of the cavern is small compared to the  $O_2$   
248 revenue. The critical factor for intermediate  $H_2$  storage is therefore not its cost, but the local availability.  
249 The sensitivity analysis proves that the cost of the electrolyzer and wind power are the main expenses in  
250 this production process. The sensitivity analysis shows that NPC ranges from 15.90  $\$/GGE$  to 21.35  $\$/$   
251  $GGE$ .

252 The effect of the interest rate, the maintenance cost, taxes, insurance expenses and the ratio factor for the  
253 chemical plant is depicted in **Fehler! Verweisquelle konnte nicht gefunden werden.**. The interest rate  
254 and the ratio factor selected for the chemical plant have the largest effect on the NPC. Depending on the  
255 assumed economic parameters, the net production cost varies by about  $\pm 5.0\%$ .

256 Cost reductions can be observed by taking the overload functionality of the PEM electrolyzer into  
257 account. An assumed overload functionality of 5.0 % of the installed capacity leads to a capital cost  
258 reduction of 3.6 %. Due to a high share of the electricity cost, the NPC is reduced by 0.9 % (18.45  $\$/$   
259  $GGE$ ). Further technology development is expected to reduce the energy demand of electrolysis to about  
260 4.1  $kWh/Nm^3$  [25], which will cut the net production cost by 4.6 % (17.77  $\$/GGE$ ). Additionally,  
261 electrolyzer capital cost is predicted to drop to about 380  $\$/kW$  [32] and electricity generation cost of  
262 offshore wind power plants may drop to 136  $\$/MWh$  [33]. Taking higher efficiency, overload  
263 capability and the predicted lower prices into account, the production cost could drop by 1/3 to about  
264 12.41  $\$/GGE$  in an optimistic future scenario (see "Future Case", **Fehler! Verweisquelle konnte nicht**  
265 **gefunden werden.**).

266 The full load capacity of the electrolyzer is highly dependent on the chosen renewable power source and  
267 its location. Hence, the outcome of the effect of the full load fraction on the net production cost is  
268 presented in **Fehler! Verweisquelle konnte nicht gefunden werden.**. With rising full load hours, the  
269 net production cost decreases due to lower expenses for the electrolyzer and the intermediate storage.

270 The share of the annual capital cost of total annual cost declines from 36 % at a full load fraction (FLF)  
271 of 10 % to about 11 % at a continuous power input (100 % FLF). The net production cost curve shows  
272 a high cost reduction potential when the FLF is increased up to 70 %.

### 273 *5.3. Fields of application and substitution potentials*

274 FT-based liquid hydrocarbons allow for a wide variety of applications. Fields of application include fuel  
275 for stationary gas turbines for power generation, in the transportation sector, or as feedstock for the  
276 chemical industry. FT-based syncrude does not fulfill the specifications for gasoline, kerosene or diesel  
277 without upgrading. They may be sold to refineries that already operate units for further processing and  
278 upgrading to transportation fuels. Alternatively, they could be used as renewable drop-in to conventional  
279 fuels. In the chemical industry, a pure feedstock is mainly required; therefore, additional distillation  
280 would be required to generate pure feedstock for further processing. Gas turbines allow for a wide  
281 variety of liquid mixtures as fuel [34]. PtL hydrocarbons provide renewable generated sulfur and  
282 nitrogen-free fuels for gas turbines. **Fehler! Verweisquelle konnte nicht gefunden werden.** compares  
283 the market feedstock prices with the calculated net production cost for the base case and a future  
284 predicted value.

285 **Fehler! Verweisquelle konnte nicht gefunden werden.** indicates that economic viability cannot be  
286 achieved for the proposed process at present. The production cost for the base case is about 7 times  
287 today's market prices of fuels and chemicals; for the future case it is about 4 times. Generation of  
288 electricity, when no renewable power is available, by using liquid hydrocarbons, which were produced  
289 from renewable electricity, reveals prices of about 4.5 times today's feedstock market prices. Taking the  
290 optimistic future case, about 3 times today's market price applies. Synthetic fuels can achieve crude oil  
291 market prices (93 \$/bbl) at power costs of 8.70 \$/MWh if electrolyzer capital cost of 380 \$/kW and a  
292 full load fraction of 100 % are assumed.

293 The net production cost ranges from 12.41 \$/GGE to 21.35 \$/GGE, depending on the assumed  
294 electricity feedstock price and electrolyzer capital cost. Strong dependence of the net production cost on  
295 the applied assumptions of the electrolyzer capital cost and the electricity price complicates the

296 comparison of the calculated costs with other studies. Becker et al. reports fuel production cost of  
297 4.66  $\$/GGE$  to 18.30  $\$/GGE$  for FLFs in the range of 20 % to 100 % and electricity prices of 20  $\$/$   
298  $MWh$  to 80  $\$/MWh$  [6]. Applying a FLF of 90 % and electricity cost of 20  $\$/MWh$ , net production  
299 cost of 5.48  $\$/GGE$  is calculated (see “20  $\$/MWh$  Case”, **Fehler! Verweisquelle konnte nicht**  
300 **gefunden werden.**), which is comparable to the reported value of 5.44  $\$/GGE$  [6]. The combination of  
301 high full load fractions and low energy prices allows the generation of liquid fuels at about twice the  
302 market prices of today (see **Fehler! Verweisquelle konnte nicht gefunden werden.**). The generation of  
303 various liquid fuels from  $H_2$  and  $CO_2$  proposing the decoupling of the  $H_2$  generation from the chemical  
304 plant was investigated [9]. Tremel et al. reports syncrude production cost of 7.50  $\$/GGE$  for FLF of  
305 70 % and a  $H_2$  feedstock price of 4  $\$/kg$ . The model of the present study determines a production cost  
306 of 8.06  $\$/GGE$  under these assumptions.

307

## 308 6. Conclusion

309 A process concept using renewable power from fluctuating wind power and  $CO_2$  to produce liquid  
310 hydrocarbons was modeled by a flowsheet simulation. The economic performance of the process was  
311 evaluated. A Power-to-Liquid efficiency of 44.6 % was calculated for a 1  $GW_{LHV}$   $H_2$  input PtL plant.

312 The economic analysis indicates that economic viability of the process cannot be achieved under current  
313 market prices for neither fuels nor chemicals. Net production cost ranges from 12.41  $\$/GGE$  to  
314 21.35  $\$/GGE$  for a wind-powered system if electrolyzer cost vary in the range of 340  $\$/kW$  to 1275  $\$/$   
315  $kW$  and the wind power cost from 136  $\$/MWh$  to 223  $\$/MWh$ . Systems with FLFs between 70 % and  
316 90 % and low electricity feedstock cost yield production costs in the range of 5.48  $\$/GGE$  to 8.03  $\$/$   
317  $GGE$ . The economic methodology underlays an inherent uncertainty of  $\pm 30$  %. Sensitivity analyses  
318 show that the main effect on the production costs comes from the electrolyzer capital cost, the wind  
319 power costs and the FLF. Therefore, reducing the costs for electrolyzer systems and electricity feedstock  
320 are the key factors for creating an economically viable production scenario of liquid hydrocarbons from  
321 renewable power and  $CO_2$ . Additionally, economic viability is more realistic for systems operating at

322 high FLFs, as they decrease the capital costs for high installed capacities of the electrolyzer and the  
323 intermediate storage. Hence, a minimum FLF of 70 % is recommended for liquid hydrocarbon processes  
324 based on renewable power.

325 The technical assessment revealed a large amount of excess heat, which is assumed to be sold. The  
326 approach of the conversion of thermal energy into electricity by a steam cycle is proposed, but this  
327 concept reveals only a small overall efficiency increase due to the low efficiency of the steam cycle. In a  
328 subsequent study, the direct thermal use of the excess heat and its effect on the process efficiency and  
329 economics will be investigated. The technical and economic potential of CO<sub>2</sub> sources will be examined  
330 to evaluate the limitations of their availability. Additionally, the technical options and the cost of  
331 upgrading products from liquid hydrocarbons to jet fuels is of special interest to the authors and will be  
332 assessed.

333



334 ACKNOWLEDGMENT

335 Financial support from the Helmholtz Association is gratefully acknowledged. This work is part

336 of the Helmholtz Energy Alliance “Synthetic Liquid Hydrocarbons”.NOMENCLATURE

337	AC	Alternate current
338	ACC	Annualized capital cost
339	ASF	Anderson-Schulz-Flory distribution
340	$\alpha$	Chain growth probability
341	CEPCI	Chemical Engineering Plant Cost Index
342	COP	Coefficient of performance
343	CSF	Carbon safety factor
344	DC	Direct current
345	EL	Electrolysis
346	$\eta_c$	Carbon conversion
347	$\eta_{CCE}$	Chemical conversion efficiency
348	$\eta_{Plant}$	Chemical plant efficiency
349	$\eta_{PtL}$	Power-to-Liquid efficiency
350	$f_{H_2+CO}$	Molar fraction of H <sub>2</sub> and CO
351	FCI	Fixed capital investment
352	FLF	Full load fraction
353	FT	Fischer-Tropsch
354	FTS	Fischer-Tropsch synthesis reactor
355	GGH	Gasoline gallon equivalent
356	$\Delta H_R^0$	Standard enthalpy of reaction ( <i>kJ/mol</i> )
357	LH	Liquid hydrocarbons
358	LHV	Lower heating value
359	LP	Low pressure steam
360	$\dot{m}$	Mass flow ( <i>t/h</i> )
361	MP	Medium pressure steam
362	n	Carbon number
363	NPC	Net production cost
364	p	Pressure ( <i>MPa</i> )
365	P	Power ( <i>MW</i> )
366	PC	Purchased cost
367	PEM	Proton exchange membrane
368	PtL	Power-to-Liquid
369	R	Recycle ratio
370	$R_{H_2/CO}$	H <sub>2</sub> -to-CO ratio
371	RWGS	High temperature reformer, reverse water gas shift reaction
372	T	Temperature ( <i>°C</i> )
373	TAC	Total annualized cost
374	TCI	Total capital investment
375	TOC	Total operation cost
376	TPC	Total purchased cost
377	w	Mass fraction

- [1] International Energy Agency, "Key World Energy Statistics," International Energy Agency, Paris, 2014.
- [2] International Energy Agency, "World Energy Investment Outlook," International Energy Agency, Paris, 2014.
- [3] P. Denholm, E. Ela, B. Kirby and M. Milligan, "The Role of Energy Storage with Renewable Electricity Generation," National Renewable Energy Laboratory, Golden, 2010.
- [4] C. Ekman and S. Jensen, "Prospects for large scale electricity storage in Denmark," *Energy Conversion and Management*, vol. 51, pp. 1140-1147, 2010. DOI:10.1016/j.econman.2009.12.023.
- [5] D. Mignard and C. Pritchard, "Processes for the synthesis of liquid fuels from CO<sub>2</sub> and marine energy," *Chemical Engineering Research and Design*, vol. 84, pp. 828-836, 2006. DOI:10.1205/cherd.05204.
- [6] W. Becker, R. Braun, M. Penev and M. Melaina, "Production of Fischer-Tropsch liquid fuels from high temperature solid oxide co-electrolysis units," *Energy*, pp. 99-115, 2012. DOI:10.106/j.energy.2012.08.047.
- [7] J. Stempien, M. Ni, Q. Sun and S. Chan, "Thermodynamic analysis of combined solid oxide electrolyzer and Fischer-Tropsch processes," *Energy*, vol. 81, pp. 682-690, 2015. DOI:10.1016/j.energy.2015.01.013.
- [8] A. Jess, P. Kaiser, C. Kern, R. Unde and C. von Olshausen, "Considerations concerning the energy demand and energy mix of global welfare and stable ecosystems," *Chemie Ingenieur Technik*, vol. 83, pp. 1777-1791, 2011. DOI:10.1002/cite.201100066.
- [9] A. Tremel, P. Wasserscheid, M. Baldauf and T. Hammer, "Techno-economic analysis for the synthesis of liquid and gaseous fuels based on hydrogen production via electrolysis," *Int. J. Hydrogen Energy*, p. in press, 2015. DOI:10.1016/j.ijhydene.2015.01.097.
- [10] O. Onel, A. Niziolek, J. Elia, R. Baliban and C. Floudas, "Biomass and Natural Gas to liquid transportation fuels and olefins (BGTL+C<sub>2</sub>\_C<sub>4</sub>): Process synthesis and global optimization," *Ind. Eng. Chem. Res.*, vol. 54, pp. 359-385, 2015. DOI:10.1021/ie503979b.
- [11] C. Zhang, K.-W. Jun, R. Gao, Y.-J. Lee and S. Kang, "Efficient utilization of carbon dioxide in gas-to-liquid process: Process simulation and techno-economic analysis," *Fuel*, vol. 157, pp. 285-291, 2015. DOI:10.1016/j.fuel.2015.04.051.
- [12] R. Kivits, M. Charles and N. Ryan, "A post-carbon aviation future: Airports and the transition to cleaner aviation sector," *Futures*, vol. 42, pp. 199-211, 2010. DOI:10.1016/j.futures.2009.11.005.
- [13] M. Carmo, D. Fritz, J. Mergel and D. Stolten, "A comprehensive review on PEM water

electrolysis," *Int. J. Hydrogen Energy*, vol. 38, pp. 4901-4934, 2013. DOI:10.1016/j.ijhydene.2013.01.151.

- [14] D. König, N. Baucks, G. Kraaij and A. Wörner, "Entwicklung und Bewertung eines Verfahrenskonzeptes zur Herstellung flüssiger Kohlenwasserstoffe unter Nutzung von CO<sub>2</sub>," *Chemie Ingenieur Technik*, no. 86, p. 1351, 2014. DOI:10.1002/cite.201450066.
- [15] A. de Klerk, Fischer-Tropsch Refining, Weinheim: Wiley-VCh Verlag, 2011. ISBN:978-3-527-32605-1.
- [16] D. Peng and D. Robinson, "A new two-constant equation of state," *Ind. Eng. Chem. Fundam.*, no. 15, pp. 59-64, 1976. DOI:10.1021/i160057a011.
- [17] J. Boston and P. Mathias, "Phase Equilibria in a Third-Generation Process Simulator," *Proceedings of the 2nd International Conference on Phase Equilibria and Fluid Properties in the Chemical Process Industries*, pp. 823-849, 17-21 March 1980.
- [18] M. Sudiro and A. Bertucco, "Production of synthetic gasoline and diesel fuel by alternative processes using natural gas and coal: Process simulation and optimization," *Energy*, no. 34, pp. 2206-2214, 2009. DOI:10.1016/j.energy.2008.12.009.
- [19] R. Baliban, J. Elia and C. Floudas, "Toward novel hybrid biomass, coal, and natural gas processes for satisfying current transportation fuel demands: 1: Process alternatives, gasification modeling, process simulation and economic analysis," *Ind. Eng. Chem. Res.*, no. 49, pp. 7343-7370, 2010. DOI: 10.1021/ie100063y.
- [20] R. Unde, "Kinetics and reaction engineering aspects of syngas production by the heterogeneously catalysed reverse water gas shift reaction," University of Bayreuth, Bayreuth, 2012.
- [21] W. Verdegaal, S. Becker and C. von Olshausen, "Power-to-Liquid: Synthetisches Rohöl aus CO<sub>2</sub>, Wasser und Sonne," *Chemie Ingenieur Technik*, vol. 87, pp. 340-346, 2015. DOI:10.1002/cite.201400098.
- [22] A. Melman and N. Woudstra, Eds., Solid oxide fuel cell systems study, Apeldoorn: Commission of the European Communities, 1991. ISBN:92-826-1960-5.
- [23] A. Steynberg and M. Dry, Eds., Fischer-Tropsch Technology, Amsterdam: Elsevier B.V., 2004. ISBN:978-0-444-51354-0.
- [24] Y. Liu, K. Murata, K. Okabe, M. Inaba, I. Takahara, T. Hanaoka and K. Sakanishi, "Selective hydrocracking of Fischer-Tropsch waxes of high-quality Diesel fuel over Pt-promoted polyoxocation-pillared montmorillonites," *Top Catal*, vol. 52, pp. 597-608, 2009. DOI:10.1007/s11244-009-9239-8.
- [25] T. Smolinka, M. Günther and J. Garche, "Stand und Entwicklungspotenzial der Wasserelektrolyse zur Herstellung von Wasserstoff aus regenerativen Energien," NOW GmbH, Berlin, 2010.
- [26] Association of the Advancement of Cost Engineering, "Cost Estimate Classification System - as applied in engineering, procurement, and construction for the process

industries," AACE International, Morgantown, 2011.

- [27] S. Towler and R. Sinnott, *Chemical Engineering Design*, Burlington: Elsevier Inc., 2008. ISBN:978-0-7506-8423-1.
- [28] M. Peters, K. Timmerhaus and R. West, *Plant Design and Economics for Chemical Engineers*, New York: McGraw-Hill, 2004. ISBN:007-124044-6.
- [29] Chemical Engineering, "Chemical Engineering Plant Cost Index," *Chemical Engineering*, p. 64, January 2015.
- [30] Y. Scholz, "Renewable energy based electricity supply at low costs: development of the REMix model and application for Europe," University of Stuttgart, Stuttgart, 2012.
- [31] C. Ainscough, D. Peterson and E. Miller, "Hydrogen production cost from PEM electrolysis," Department of Energy USA, Washington, DC, 2014.
- [32] J. Levene, B. Kroposki and G. Sverdrup, "Wind energy and production of hydrogen and electricity - opportunities for renewable hydrogen," National Renewable Energy Laboratory, Golden, 2006.
- [33] International Energy Agency, "Technology Roadmap Wind energy," International Energy Agency, Paris, 2013.
- [34] C. Soares, *Gas Turbines*, Oxford: Butterworth-Heinemann, 2015. ISBN:978-0-12-410461-7.
- [35] G. Saur, "Wind-to-hydrogen project: electrolyzer capital cost study," National Renewable Energy Laboratory, Golden, 2008.
- [36] O. van Vliet, A. Faaij and W. Turkenburg, "Fischer-Tropsch diesel production in a well-to-wheel perspective: A carbon, energy flow and cost analysis," *Energy Conversion Management*, vol. 50, pp. 855-876, 2009. DOI:10.1016/j.enconman.2009.01.008.
- [37] D. Steward, G. Saur, M. Penev and T. Ramsden, "Lifecycle cost analysis of hydrogen versus other technologies for electrical energy storage," National Renewable Energy Laboratory, Golden, 2009.
- [38] U.S. Energy Information Administration, "www.eia.gov," 2015. [Online]. Available: <http://www.eia.gov/dnav/pet/hist/LeafHandler.ashx?n=pet&s=rwtc&f=m>. [Accessed 31 03 2015].
- [39] Platts, "Solventswire," The McGraw-Hill, Houston, vol. 35. 2012.
- [40] U.S. Energy Information Administration, "www.eia.gov," 2015. [Online]. Available: [http://www.eia.gov/dnav/pet/pet\\_pri\\_gnd\\_dcus\\_nus\\_a.htm](http://www.eia.gov/dnav/pet/pet_pri_gnd_dcus_nus_a.htm). [Accessed 31 03 2015].
- [41] P. Kaiser, F. Pöhlmann and A. Jess, "Intrinsic and effective kinetics of cobalt-catalyzed Fischer-Tropsch synthesis in view of a Power-to-Liquid process based on renewable energy," *Chemical Engineering Technology*, vol. 37, pp. 964-972, 2014. DOI:10.1002/ceat.201300815.

- [42] R. Swanson, A. Platon, J. Sapiro and R. Brown, "Techno-economic analysis of Biomass-to-Liquids production based on gasification," *Fuel*, vol. 89, pp. 11-19, 2010. DOI:10.1016/j.fuel.2010.07.027.
- [43] Dutch Association of Cost Engineers, Price Booklet, vol. 30, Den Haag: BIM Media, 2014. ISBN: 978-94-62-45051-6.
- [44] P. Markussen, J. Austell and C. Hustad, "A CO<sub>2</sub>-infrastructure for EOR in the North Sea (CENS): Macroeconomic implications for host countries," *Sixth Int. Conference on Greenhouse Gas Control Technologies*, vol. 324, 2002.
- [45] G. Ulrich and P. Vasudevan, "How to estimate utility costs," *Chemical Engineering*, pp. 66-69, 2006.
- [46] P. Rao and M. Muller, "Industrial oxygen: its generation and use," *ACEEE Summer Study on Energy Efficiency in Industry*, vol. 6, pp. 124-135, 2007.

380

381

382 References [43] to [46] refer to citations in the supplementary information (Table S3).